0026-895X/01/5903-475–485$3.00
MOLECULAR PHARMACOLOGY
Copyright © 2001 The American Society for Pharmacology and Experimental Therapeutics
Mol Pharmacol 59:475–485, 2001

Vol. 59, No. 3
502/887118
Printed in U.S.A.

Amino Acid Residues Critical for Differential Inhibition of CYP2B4, CYP2B5, and CYP2B1 by Phenylimidazoles

MARGIT SPATZENEGGER, QINMI WANG, YOU QUN HE, MICHAEL R. WESTER, ERIC F. JOHNSON, and JAMES R. HALPERT

Department of Pharmacology and Toxicology, University of Texas Medical Branch, Galveston, Texas (M.S., Q.W., Y.Q.H., J.R.H.); Department of Molecular and Experimental Medicine, The Scripps Research Institute, La Jolla, California (M.R.W., E.F.J.)

Received August 18, 2000; accepted November 2, 2000

This paper is available online at http://molpharm.aspetjournals.org

ABSTRACT

The molecular basis for reversible inhibition of rabbit CYP2B4 and CYP2B5 and rat CYP2B1 by phenylimidazoles was assessed with active-site mutants and new three-dimensional models based on the crystal structure of CYP2C5. 4-Phenylimidazole was 17- to 32-fold more potent toward CYP2B4 and CYP2B1 than CYP2B5. The 3D models, along with site-directed mutagenesis data, revealed the importance of residue 114 for sensitivity to inhibition of all three CYP2B enzymes. Besides Ile 114, Val 367 was also found to be critical for inhibition of CYP2B4 and CYP2B1. The most interesting new insights were obtained from analysis of the CYP2B5 model and the CYP2B5 active-site mutants. Simultaneous substitution of residues 114, 294, 363, and 367 with the corresponding residues of CYP2B4 decreased the IC_{50} value for inhibition by 4-phenylimidazole 12-fold. Docking 4-phenylimidazole into the models of CYP2B5 mutants demonstrated that the inhibitor-binding site is strongly influenced by residue-residue interactions, especially between residues 114 and 294. A chlorine substitution at position 4 of the phenyl moiety of 4- and 1-phenylimidazole resulted in IC_{50} values 95- and 130-fold lower for CYP2B4 than for CYP2B5, respectively, suggesting that these compounds are selective inhibitors of CYP2B4. Overall, the study revealed that differences in the determinants of inhibition between CYP2B4 and CYP2B5 are caused not only by single residue inhibitor contacts but also by residue-residue interactions. This new generation of CYP2B models may provide valuable information for the design of selective inhibitors of human CYP2B6 and for the development of drugs that avoid drug interactions due to P450 inhibition.

A major challenge in the drug discovery process is the ability to predict catalytic specificities of individual P450 enzymes. Selective inhibitors are crucial for the identification of P450 enzymes involved in biotransformation (Halpert, 1995). One approach to finding P450 inhibitors is in vitro screening of compounds using microsomes or heterologous expression systems (Pelkonen et al., 1998). Another strategy is developing active-site mutants and homology models of the enzymes. This more theoretical approach has the advantage of being applicable to virtual screening of compounds not yet synthesized. Furthermore, this method provides detailed knowledge of the molecular basis of inhibition and facilitates the drug discovery process through prediction of suitable structural alterations that minimize potential drug-drug interactions caused by P450 inhibition but maintain pharmacological activity. In the absence of an experimental structure, models of mammalian P450s have been constructed by homology with bacterial P450s of known crystal structure (Szklarz et al., 1995; Lewis, 1998; de Groot et al., 1999; Payne et al., 1999; Dai et al., 2000). Models based on bacterial enzymes such as CYP102 have been used to pinpoint key residues that may be important for substrate specificity (Lewis and Lake, 1997). Furthermore, the analysis of interactions between single active-site residues and the substrate has facilitated the understanding of regio- and stereospecificity of substrate oxidation as well as susceptibility to inhibition or inactivation (Szklarz et al., 1995; Chang et al. 1997). However, the low sequence identity of mammalian P450s compared with the bacterial enzymes has limited progress.

Rat CYP2B1 and rabbit CYP2B4 and CYP2B5 provide an excellent basis to study the structural determinants of inhibition. These 2B enzymes have been extensively studied by molecular modeling (Szklarz et al., 1995; Chang et al., 1997; Lewis and Lake, 1997; Dai et al., 1998) and site-directed mutagenesis. Studies in our laboratory have revealed that residues 114, 206, 209, 290, 294, 302, 363, 367, 477, 478, and 480, which are located in five different substrate recognition sites (SRSs), control specificities toward various substrates such as androstenedione, progesterone, pentoxyresorufin,

This work was supported by AstraZeneca and National Institutes of Health Grants ES03619 (J.R.H.), GM31001 (E.F.J.), and Center Grant ES06676. An abstract of this work appeared in *FASEB J* **14:**158.

ABBREVIATIONS: P450, cytochrome P450; SRS, substrate recognition site; CHAPS, 3-[(3-cholamidopropyl)dimethylammonio]-1-propanesulfonic acid; BROD, benzyloxyresorufin *O*-debenzylase; PROD, pentoxyresorufin *O*-dealkylase; WT, wild-type.

benzyloxyresorufin, 7-ethoxycoumarin, and benzphetamine (He et al., 1992, 1994, 1995; Szklarz et al., 1996; Kobayashi et al., 1998). CYP2B4 and CYP2B5 are especially intriguing, because they differ in only 12 amino acid residues but exhibit different catalytic selectivities. Four amino acid residues [those at position 114 (SRS-1), 294 (SRS-4), and 363 and 367 (SRS-5)] have been identified as crucial for distinct activities of CYP2B4 and CYP2B5 (He et al., 1996; Szklarz et al., 1996). Recently, the structural basis for selective CYP2B4 and CYP2B5 inactivation was assessed using active-site mutants and homology modeling. 2-Ethynylnaphthalene was identified as a selective inactivator of CYP2B4 but not of CYP2B5. In molecular dynamic simulations, 2-ethynylnaphthalene was stable within the CYP2B4 model but exhibited significant movement away from the heme moiety in the CYP2B5 model. Interconversion of 2-ethynylnaphthalene susceptibility was achieved for CYP2B4 and CYP2B5 by a single alteration at position 363 (Strobel et al., 1999). However, the mechanism-based inactivation process is complex, and elucidation of the molecular basis of reversible inhibition would be of great interest.

Some of the most potent reversible inhibitors of P450 enzymes are the nitrogen heterocycles, including imidazoles and quinolines. P450 inhibition by these compounds results from direct interaction between the aromatic nitrogen of the heterocycle and the heme moiety of the enzyme (Murray, 1987). X-ray crystallographic studies of bacterial $P450_{cam}$ complexed with 1-, 2- or 4-phenylimidazole have demonstrated that a sterically accessible lone electron pair provided by the heterocyclic nitrogen atom is required for heme iron coordination (Poulos and Howard, 1987). Furthermore, type II binding studies of phenylpyridines, phenylimidazoles, and pyridylimidazoles to cytochrome P450 in hepatic microsomes from phenobarbital-induced rats showed the highest binding affinity for compounds in which steric hindrance near the nitrogen was minimal (Murray and Wilkinson, 1984). Therefore, phenylimidazoles promised to be valuable probes for studying the molecular basis of differential P450 inhibition.

This study identifies specific active-site residues critical for differential sensitivity to inhibition of CYP2B4, CYP2B5, and CYP2B1 by phenylimidazoles. The recent elucidation of the crystal structure of rabbit CYP2C5 (Williams et al., 2000) provided an invaluable template for construction of a new generation of homology models of the CYP2B enzymes. These models and inhibition studies of active-site mutants with 4-phenylimidazole revealed that residues 114, 294, 363, and 367 are critical for CYP2B4, CYP2B5, and CYP2B1 inhibition. The results provide novel insight into residue-residue interactions in the active site that confer differential inhibition sensitivity and catalytic selectivity of the CYP2B enzymes.

Experimental Procedures

Materials. Restriction endonucleases, Luria-Bertani Broth and Terrific Broth media for bacterial growth were purchased from Life Technologies (Grand Island, NY). The *Escherichia coli* strain Topp3 was obtained from Stratagene (La Jolla, CA). Androstenedione, resorufin, 7-benzyloxyresorufin, 7-pentoxyresorufin, NADPH, dimethyl sulfoxide, dilauroyl-L-3-phosphatidylcholine, CHAPS, δ-aminolevulinic acid, isopropyl β-*d*-thiogalactopyranoside, 1-(2-trifluoromethylphenyl)imidazole and BioMax MR-1 film were purchased from Sigma Chemical Co. (St. Louis, MO). HEPES was obtained from Calbiochem Co. (La Jolla, CA). [^{14}C]Androstenedione was purchased from DuPont-NEN (Boston, MA). Thin-layer chromatography plates [silica gel, 250 μm, Si 250PA (19C)] were obtained from J.T. Baker, Inc. (Phillipsburg, NJ). Rat NADPH cytochrome P450 reductase was expressed in *E. coli* as described previously (Harlow and Halpert, 1997). 1-Phenylimidazole, 4-phenylimidazole, 1-benzylimidazole, 2-methylimidazole, 2-phenylimidazole, and 1-(2,3,5,6-tetrafluorophenyl)imidazole were obtained from Aldrich Chemical Co. (Milwaukee, WI). 4-(4-Chlorophenyl)imidazole was purchased from Maybridge Chemical Company (Tintagel Cornwall, UK), and 1-(4-chlorophenyl)imidazole was obtained from Lancaster (Pelham, NH). All other chemicals and supplies used were from standard sources.

Subcloning of P450 2B1 Mutants and Heterologous Expression. cDNA encoding CYP2B1 V367L was previously subcloned into the pBC vector yielding pBC2B1 V367L (He et al., 1994). For expression in *E. coli*, the cDNA 2B1 V367L was subcloned into pKK2B1 (He et al., 1995). pBC2B1 V367L was digested with the unique restriction enzymes *Hin*dIII and *Pst*I. The appropriate fragment was purified by GeneClean II (Bio 101, Vista, CA) and ligated into purified pKK2B1, which was also digested with *Hin*dIII and *Pst*I. To construct pKK2B1 L58F/I114F, plasmid $pSE2B2_{FF}$ (L58F-I114F) (Strobel and Halpert, 1997) was digested with *Pst*I and *Kpn*I, and the resulting fragment was subsequently subcloned into pKK2B1. The triple mutant CYP2B1 L58F-I114F-S294T was constructed by digesting pKK2B1 L58F-I114F and pKK2B1 S294T with *Bam*HI. The fragment containing the mutations of L58F-I114F was ligated into phosphatase-treated pKK2B1 S294T and transformed into *E. coli* DH5α cells. All plasmids were identified by restriction mapping and/or sequencing (373 XL ABI DNA sequencer; ABI, Norwalk, CT). All other mutants tested in this study were constructed previously (He et al., 1995, 1996; Szklarz et al., 1996; Strobel and Halpert, 1997). *E. coli* Topp3 cells were transformed with pKK2B4, pKK2B5, pKK2B1, and pSE2B2 wild-type and mutant plasmids. Conditions for expression were as described earlier (John et al., 1994). CHAPS-solubilized membranes were prepared as described previously (John et al., 1994). Total P450 concentration was measured by reduced CO difference spectra (Omura and Sato, 1964).

Spectral Binding Studies. Difference spectra were recorded on a Shimadzu UV-2600 spectrophotometer at 37°C. A solution of 0.4 μM CYP2B1 WT and CYP2B1 mutants in a buffer containing 100 mM MOPS and 10% glycerol, pH 7.3, was prepared and divided into two 0.5-ml quartz cuvets (1-cm path length), and a baseline was recorded between 350 and 500 nm. An aliquot of inhibitor in methanol was then added to the sample cuvette, and the same amount of methanol was added to the reference cuvette. The difference spectra were obtained after the system reached equilibrium (3 to 5 min). The spectral dissociation constants (K_D) were obtained by fitting the data to the equation for "tight binding" $\Delta A = ((K_D + [I_0] + [E_0]) - ((K_D + [I_0] + [E_0]))^2 - 4[E_0][I_0])^{1/2}) / 2$ when $K_D \leq 4$ μM or to the conventional equation $\Delta A = [I][E_0] / (K_D + [I])$ (Copeland, 2000).

Inhibition Studies. Inhibition studies were carried out with 7-benzyloxyresorufin, 7-pentoxyresorufin, or androstenedione as substrates. Some of the mutants of CYP2B4 and CYP2B5 showed very low activity for one or two of these substrates. To achieve the most exact IC_{50} values, the substrate yielding the highest activity was chosen in each case. Benzyloxyresorufin *O*-debenzylase (BROD) activities were measured for CYP2B1 and all CYP2B1 mutants, for CYP2B4, the CYP2B4 single mutants, and the CYP2B5 F114I-T294S-V363I-A367V quadruple mutant. Activities of CYP2B5, the CYP2B5 single mutants, and the CYP2B4 I114F-S294T-I363V-V367A quadruple mutant were determined by the pentoxyresorufin *O*-dealkylase (PROD) assay. Androstenedione was used to investigate the inhibition of all double and triple mutants of CYP2B4 and CYP2B5. BROD, PROD, and androstenedione hydroxylase activities were determined as described previously (He et al., 1995). Inhibitors were added from a 100× methanol stock solution (final methanol concentration was ≤ 0.7%). Control reactions without inhibitor were performed by adding the same amount of methanol. The final 500-μl

reaction mixture contained 20 pmol of P450 to determine BROD activity (linear from 5–25 pmol) and 15 pmol of P450 to determine PROD activity (linear from 5–17.5 pmol). Both substrates were used at a concentration of 10 μM. Preliminary studies showed linearity of resorufin formation up to 15 min incubation time at 37°C for BROD activity and up to 7.5 min for PROD activity; thus the reactions were stopped with methanol after 10 and 5 min, respectively. For the androstenedione hydroxylase assay, 10 pmol of P450 were used in a final 100-μl reaction mixture. The reaction was stopped with tetrahydrofuran after 15-min incubation and metabolites were resolved on TLC plates (He et al., 1995). The half-maximal inhibitor concentrations (IC_{50}) were obtained from the mean inhibition observed at five or more different inhibitor concentrations in two separate determinations performed in duplicate. IC_{50} values were calculated by linear regression analysis of the degree of inhibition as a function of inhibitor concentration (Augustinsson, 1948). The degree of inhibition was expressed as the ratio of the reaction rates of uninhibited and inhibited enzyme. The graph directly gives the IC_{50} value as the molar concentration of the inhibitor when $V_0/V_{inhibitor} = 2$ (V_0 = uninhibited reaction rate; $V_{inhibitor}$ = inhibited reaction rate). A difference between IC_{50} values of at least 2-fold was considered significant.

Computer Modeling. Molecular models were constructed using the InsightII software package (Homology/InsightII, Discover_3/InsightII, Biopolymer/InsightII, and Docking/InsightII from Molecular Simulations Inc., San Diego, CA). The CYP2B models were constructed based on the crystal structure of CYP2C5 (pdb accession number: 1dt6 on hold) (Cosme and Johnson, 2000). The sequences of CYP2B1, CYP2B4, and CYP2B5 were obtained from SwissProt (accession numbers P00176, P00178, and P12789, respectively). The sequence alignment of CYP2C5, CYP2B1, CYP2B4, and CYP2B5 was done by GCG (Wisconsin Package Version 10.0; PileUp; Genetics Computer Group, Madison, WI). In the crystal structure of CYP2C5, the coordinates for the N-terminal residues 1 to 30 and the F-G loop residues 212 to 222 were missing. Therefore, the models were constructed from residues 31 to 491. The segment between residues 212 and 222 was modeled based on the coordinates of CYP2C5 containing one of two alternative models for density corresponding to the F-G loop (E.F.J., unpublished observations). The coordinates of residues 276 to 278, the only segment not considered to be conserved, were generated using the random tweak method in Homology/InsightII (Shenkin et al., 1987) (Fig. 2). The coordinates of the conserved residues were assigned based on the corresponding residues of CYP2C5 by Homology/InsightII. The heme group was copied from CYP2C5 into the CYP2B models.

After the coordinate assignment, the preliminary 3D structures of CYP2B1, CYP2B4, and CYP2B5 were refined. Energy minimization was performed by Discover_3 using a consistent valence force field. The parameters for the heme group were described previously (Paulsen and Ornstein, 1991, 1992). The cvff force field encoded in InsightII was used for the other part of the enzyme. First, splices between residues 211 and 212, 222 and 223, 275 and 276, and 278 and 279 were repaired by Homology/InsightII to avoid steric hindrance in these junction regions. All hydrogen atoms were minimized by fixing the heavy atoms of the 2B enzymes. The side chains were minimized by fixing the backbone. A 25-Å sphere and 3-Å surface layer of water were soaked into and around the minimized protein with the SOAK function in Viewer/InsightII. Energy minimization was performed again on the whole soaked enzyme. For the 2B5 mutants, the coordinates of the corresponding residues were changed in the 2B5 3D model by Biopolymer/InsightII, and the resulting 2B5 mutants were minimized.

The quality of the models was checked by Prostat/InsightII, which allows protein specific bond lengths, angles, and torsions to be checked against the corresponding reference values. The cutoff used, which represents the significant difference for bond length, bond angle, and torsion from the reference value, is 5 S.D. For the 2B1 model, none of the bond distances, one bond angle, and five dihedral angles were identified to have more than 5 S.D. For the 2B4 model, none of the bond distances, three bond angles, and seven torsions had more than 5 S.D. For the 2B5 model, none of the bond distances, five bond angles, and 11 dihedral angles have more than 5 S.D.

4-Phenylimidazole was manually docked into the 3D models of CYP2B1, CYP2B4, CYP2B5, and CYP2B5 mutants. The initial position of 4-phenylimidazole in the active site of these enzymes was determined from the position of 4-phenylimidazole in the active site of $P450_{cam}$ after superimposing the heme groups. The crystal structure of the 4-phenylimidazole-$P450_{cam}$ complex was obtained from the Brookheaven Protein Databank (1PHF; Poulos and Howard, 1987), where the distance between the nitrogen atom of 4-phenylimidazole (N) and the heme iron (Fe) was 2.2 Å. Energy minimizations were performed on the 4-phenylimidazole CYP2B complexes. During the minimization process, the Fe-N distance was fixed at 2.2 Å to maintain the coordinate bond. For each CYP2B enzyme, possible orientations of the imidazole ring and of the phenyl ring of 4-phenylimidazole were examined separately. A series of initial orientations of the imidazole ring were constructed where the ring was fixed every 30° in a 360° rotation. Regardless of the initial orientation, molecular mechanics minimization of each of these structures invariably placed the imidazole ring in one of two positions that were related to each other by a rotation of approximately 180° degrees. In one of these positions, the phenyl ring points to a portion of the active site distant from the key residues 114, 294, and 367, which is inconsistent with experimental results and was disregarded. The other position is shown in Fig. 3, A, B, and D. A series of initial orientations of the phenyl ring was also constructed. The ring was oriented every 30° in a 180° rather than 360° rotation because of the C2 symmetry of the phenyl ring. Only one position was obtained in each CYP2B enzyme after molecular mechanics minimization on these initial structures, as shown in Fig. 3, A, B, and D.

Results

Inhibitor Selection and Basic Experimental Approach. An initial screening of CYP2B4 and CYP2B5 inhibition using different phenylimidazole compounds revealed 4-phenylimidazole as a selective inhibitor for CYP2B4. Inhibition of CYP2B4 activity by 4-phenylimidazole was 18-fold more potent than that of CYP2B5 activity (Fig. 1A). The IC_{50} values of 1-, 2-, and 4-phenylimidazole for CYP2B4 were 0.9 μM, 1.8 mM, and 0.49 μM, respectively. These data are consistent with other reports (Murray and Wilkinson, 1984) and showed that the affinity of phenylimidazoles is largely dependent on the accessibility of the nitrogen atom of the heterocycle, which is impaired with 2-phenylimidazole. Because 4-phenylimidazole showed significantly different inhibition effects on CYP2B4 and CYP2B5 activity and the highest binding affinity, further investigations of the molecular requirements for inhibition were performed with 4-phenylimidazole.

Because of the need to study a large number of CYP2B mutants, IC_{50} values were used to evaluate the potency and affinity of binding of the phenylimidazole compounds. Earlier investigations with rat liver microsomes showed a striking correlation between the K_D values and the IC_{50} values for phenylimidazole compounds (Murray and Wilkinson, 1984). This finding reflects the dominance of the strong coordinate bond between the heme iron of cytochrome P450 and the nitrogen of the imidazole ring of the phenylimidazole compound in determining inhibitor potency. To ensure that neither different substrates nor different substrate concentrations had a significant effect on inhibitor potency, IC_{50} values of 4-phenylimidazole for CYP2B4 WT and CYP2B5 WT were

determined under a variety of conditions. The IC_{50} values of 4-phenylimidazole for CYP2B4 WT determined by three assays differed only insignificantly (BROD, IC_{50} = 0.49 μM; PROD, IC_{50} = 0.46 μM; androstenedione hydroxylase activity: IC_{50} = 0.3 μM) (Fig. 1B). Similar results were observed for CYP2B5 WT when 7-pentoxyresorufin and androstenedione were used as substrates (PROD, IC_{50} = 8.4 μM; androstenedione hydroxylase activity, IC_{50} = 10.6 μM). Moreover, in a separate experiment, the IC_{50} for inhibition of CYP2B4 WT activity by 4-phenylimidazole was constant over a 10-fold range of 7-benzyloxyresorufin concentrations (data not shown). Finally, inhibition of CYP2B5 by 4-phenylimidazole using androstenedione as a substrate indicated virtually noncompetitive inhibition, as shown in Fig. 1C. Based on all these findings, IC_{50} values were used in subsequent experiments as a measure of inhibitor potency.

Differential Sensitivity of CYP2B4 and 2B5 to Inhibition by 4-Phenylimidazole and Analysis of Active-Site Mutants. To assess the structural basis of differential sensitivity of CYP2B4 and CYP2B5, inhibition studies were performed with active-site mutants. Based on recent findings of the importance of residues 114, 294, 363, and 367 for substrate specificities of CYP2B4 and CYP2B5, mutants containing alterations at these positions were tested. These mutants had been previously constructed (He et al., 1996; Szklarz et al., 1996). Because of low basal activities, inhibition of the CYP2B4 I114F and CYP2B5 F114I enzymes could not be determined.

In CYP2B4, substitutions of the single residues 294 and 363 with those of CYP2B5 did not change the IC_{50} value significantly (Table 1). However, the Val 367-to-Ala substitution decreased the sensitivity to inhibition by 4-phenylimidazole substantially. Increased IC_{50} values were observed for the single mutant CYP2B4 V367A (7-fold) as well as for the double mutant CYP2B4 I363V-V367A (20-fold) compared with the WT. The sensitivities to inhibition of both mutants were similar to that of I114F-S294T-I363V-V367A, suggesting that the replacement of residue 367 with Ala might be responsible for the low sensitivity to inhibition of the quadruple mutant. However, residue 114 was also important for inhibition. The I114F-S294T mutant showed a 50-fold higher IC_{50} value compared with the WT and a 35-fold higher IC_{50} value than S294T. The simultaneous replacement of Ile 114, Ile 363, and Val 367 with Phe, Val, and Ala, respectively,

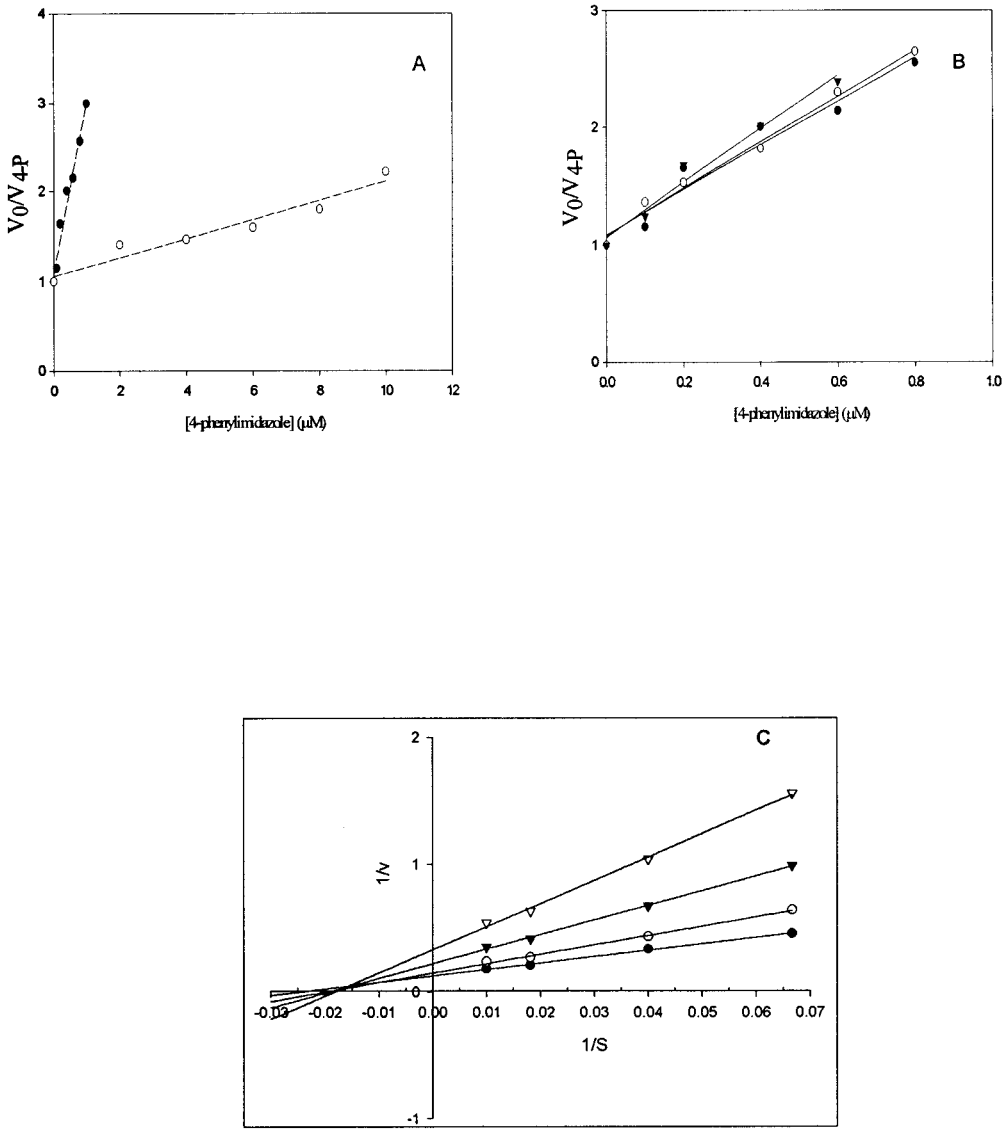

Fig. 1. A, inhibition of CYP2B4 (●) and CYP2B5 (○) by 4-phenylimidazole. B, inhibition of CYP2B4 determined with three substrates. The IC_{50} value was determined by the inhibition of BROD (●), PROD (○), and androstenedione hydroxylase (▼) activity as described under *Experimental Procedures*. The lines shown were generated by linear regression ($r^2 > 0.96$). The IC_{50} values are given as the micromolar concentration of 4-phenylimidazole when $V_0/V_{4\text{-P}}$ = 2. C, Lineweaver-Burk plot of the inhibition of the androstenedione 16α-hydroxylase activity of CYP2B5 WT by 4-phenylimidazole. K_i, 10.8 ± 0.8 μM; K_m, 40.3 ± 5.1 μM; V_{max}, 8.1 ± 0.5 nmol/min/nmol CYP2B5 WT. Data were calculated with the equation for noncompetitive inhibition: $v = V_{max}[S]/((([S] + K_m)(1 + [I]/K_i))$; ●, no inhibitor; ○, 5 μM 4-phenylimidazole; ▼, 10 μM 4-phenylimidazole; ▽, 20 μM 4-phenylimidazole.

TABLE 1
Inhibition of CYP2B4 enzymes by 4-phenylimidazole
IC_{50} values are the means of two independent experiments performed in duplicate and conducted as described under *Experimental Procedures*.

P450	IC_{50}
	μM
WT	0.49[a]
S294T	0.65[a]
I363V	0.93[a]
I114F-I363V-V367A	1.8[b]
V367A	3.4[a]
I363V-V367A	9.7[b]
I114F-S294T	22.5[b]
I114F-S294T-I363V-V367A	7.2[c]

[a] Values determined by BROD assay.
[b] Values determined by androstenedione hydroxylase assay.
[c] Values determined by PROD assay.

TABLE 2
Inhibition of CYP2B5 enzymes by 4-phenylimidazole
Values are the means of two independent experiments performed in duplicate and conducted as described under *Experimental Procedures*.

P450	IC_{50}
	μM
WT	8.4[c]
T294S	87[c]
F114I-T294S	22[b]
V363I	8.8[c]
A367V	6.6[c]
T294S-V363I-A367V	6.2[b]
V363I-A367V	5.8[b]
F114I-V363I-A367V	2.3[b]
F114I-T294S-V363I-A367V	0.69[a]

[a] Values determined by BROD assay.
[b] Values determined by androstenedione hydroxylase assay.
[c] Values determined by PROD assay.

resulted in only a 3.7-fold increase of the IC_{50} value compared with the WT. Overall, the inhibition studies with the various mutants showed the important role of the side chains of residue 367 and 114 in high inhibitor sensitivity.

In CYP2B5, single substitutions of Val 363 and Ala 367, as well as simultaneous replacement of Val 363 and Ala 367 with the corresponding residues of CYP2B4, did not change sensitivity to inhibition substantially (Table 2). Although the single mutant F114I showed insufficient activity for inhibition studies, simultaneous substitutions with other residues pointed out that this residue plays a crucial role in inhibitor sensitivity. When Phe 114 and Thr 294 were replaced by Ile and Ser simultaneously, the IC_{50} value decreased about 4-fold compared with T294S alone. Likewise, F114I-V363I-A367V exhibited a 2.5-fold decrease in the IC_{50} value compared with the V363I-A367V mutant. Moreover, when the Phe 114-to-Ile substitution was added to the triple mutant T294S-V363I-A367V, the IC_{50} value showed a 9-fold decrease. Substitutions of residue 294 raised the intriguing question that the molecular basis of inhibitor sensitivity of CYP2B5 involves the rearrangement of several active-site residues. The single replacement of Thr 294 by Ser in CYP2B5 WT led to a 10-fold increase in the IC_{50} value. However, when residue 294 was substituted with Ser in the V363I-A367V mutant, no significant change of the IC_{50} value was observed. Finally, the addition of a Thr 294-to-Ser substitution to the triple mutant F114I-V363I-A367V decreased the IC_{50} value significantly. These mutagenesis data revealed that the architecture of the inhibitor-binding site of CYP2B5 may be defined by complex interactions among the active-site residues, especially residues 114 and 294.

Sensitivity of CYP2B1 to Inhibition by 4-Phenylimidazole and Analysis of the Active Site Mutants. It was of great interest to ascertain whether the findings regarding the molecular requirements for CYP2B4 and CYP2B5 inhibition could be extrapolated to rat CYP2B1. Furthermore, the investigation of inhibitor sensitivity of CYP2B1 allowed us to analyze the importance of certain active-site residues more carefully. With an additional substitution of the nonactive site Leu 58 with Phe, the CYP2B1 I114F mutant expressed sufficiently to obtain reasonable activity. The inhibition of CYP2B1 WT activity by 4-phenylimidazole resulted in a low IC_{50} value, similar to that observed for CYP2B4 WT (Table 3). Spectral studies of 4-phenylimidazole binding to CYP2B1 WT and selected mutants indicated a strong correlation between K_D values and IC_{50} values, confirming the pivotal role of the Fe-N bond for inhibition (Table 3). The tight type II binding of 4-phenylimidazole to CYP2B1 WT (K_D = 0.3 ± 0.1 μM) was in strong contrast to the weak type I binding of 2-phenylimidazole (K_D= 1.5 ± 0.2 mM). Substitution of Val 363 with Ala or of Ser 294 with Ala or Thr caused almost no change in sensitivity to inhibition. However, a Val 363-to-Leu substitution led to a decrease of almost 3-fold in the IC_{50} value. Similar to the findings with CYP2B4, substitution of Val 367 with Ala increased the IC_{50} value 23-fold, whereas the mutation of this residue to Leu decreased the IC_{50} value 6-fold compared with the WT. Furthermore, the substitution of Leu 58 and Ile 114 with Phe increased the IC_{50} value 130-fold compared with the WT.[1] Strikingly, the replacement of Ser 294 with Thr in 2B1 L58F-I114F resulted in an 85-fold decrease in the IC_{50} value back to wild-type levels. In conclusion, interesting similarities between the results of CYP2B1 and CYP2B4 inhibition were observed. Besides, the importance of residue 114 for sensitivity to inhibition the construction of the mutants CYP2B1 L58F-I114F and CYP2B1 L58F-I114F-S294T suggested an interaction between residues 114 and 294, as noted in CYP2B5.

Modeling of CYP2B1, CYP2B4, CYP2B5, and Mutants and Docking of 4-Phenylimidazole into the Active Site. The docking of 4-phenylimidazole into models constructed based on the crystal structure of bacterial P450s (Szklarz et al., 1996) was uninformative. Therefore, 2B models were constructed based on the coordinates of the recently solved CYP2C5 crystal structure (Williams et al., 2000). The sequence alignment used for modeling CYP2B1, CYP2B4, and CYP2B5 is summarized in Fig. 2. This sequence alignment was performed by GCG except for the insertion between 274Q and 280N (QEN. . . N), which was changed to QE. . . NN after the analysis of the CYP2C5 structure. This alteration allows room for the insertion without disrupting the structure.

In the CYP2B4 model, the side chains of Ile 114, Val 367,[2] and Ile 363 lie within 5 Å of 4-phenylimidazole (Fig. 3A). Residues Ile 114 and Val 367 were the closest to 4-phenylimidazole at 3.8 Å and 3.9 Å, respectively. Ile 363 and Ser

[1] A very similar effect was observed in CYP2B2 when Leu 58 and Ile 114 were replaced simultaneously with Phe residues. The IC_{50} value of 4-phenylimidazole increased from 0.8 μM for the wild-type enzyme to 44 μM for CYP2B2 L58F-I114F.
[2] The distances reported under *Results* are those between the nearest atoms of the residue and 4-phenylimidazole.

294 lie 4.4 Å and 6.2 Å away from the docked molecule, respectively. The proximity of residues 114 and 367 to the phenyl moiety of 4-phenylimidazole could explain the importance of those residues for inhibition of CYP2B4. In contrast to the CYP2B4 model, the CYP2B5 model revealed that Phe 114 and Thr 294 are located 3.6 Å and 3.7 Å from the docked compound (Fig. 3B). The residues Val 363 and Ala 367 are 5.7 Å and 7.8 Å away from 4-phenylimidazole. Furthermore, the architecture of the active site seems to be influenced by interaction between the residues Phe 114 and Thr 294, which are located in the B′-C-loop and in the I-helix, respectively (Fig. 3C).

Models of CYP2B5 mutants with 4-phenylimidazole docked into the active site revealed significant changes in the position of 4-phenylimidazole and in the distances of the active-site residues from the compound, partially because of compensatory movements of the I-helix and the B′-C-loop (Fig. 4). The single substitution of Thr 294 with Ser led to the movement of the phenyl ring of Phe 114 toward Ser 294 and subsequently disrupted the π-stacking of the phenyl ring of Phe 114 with the phenyl moiety of 4-phenylimidazole (Fig. 4A). The additional substitution of Phe 114 to Ile resulted in more space for 4-phenylimidazole and in movement of the phenyl ring of 4-phenylimidazole toward residues 363 and 367 (Fig. 4B). Substitutions of Val 363 and Ala 367 with the larger residues Ile and Val, as shown in Fig. 4C, decreased the distances of these residues to 4-phenylimidazole. Because of the additional replacement of Thr 294 with the smaller Ser, the phenyl ring of Phe 114 moved closer to Ser 294, and the phenyl moiety of 4-phenylimidazole moved closer to residue 363 (Fig. 4D). However, a significant alteration in the position of the phenyl ring of 4-phenylimidazole was only observed when Phe 114, Val 363, and Ala 367 were simultaneously substituted with Ile, Ile, and Val, respectively (Fig. 4E). Consequently, residues 363 and 367 are located within 5 Å of 4-phenylimidazole. When all four residues were simultaneously replaced by the corresponding residues of CYP2B4, the distances between the residues from 4-phenylimidazole were similar to those in the CYP2B4 WT model with the exception of Val 367, which was 1.2 Å farther away from 4-phenylimidazole than in the CYP2B4 WT model (Fig. 4F). These detailed observations of CYP2B5 mutants with 4-phenylimidazole docked into the active site reveal an intriguing interplay between active-site residues, which is consistent with the complex experimental data, especially for residues 114 and 294. These residue-residue interactions might strongly influence the potency of inhibition of CYP2B5.

In the CYP2B1 model, the side chain of Val 367 is 3.6 Å away from 4-phenylimidazole (Fig. 3D). Ile 114 is 4.4 Å away from the inhibitor molecule. Ser 294 and Val 363 are positioned more than 6 Å away from the compound. The distances of the residues from 4-phenylimidazole are similar to those observed in CYP2B4 except for residue 363, which is closer to the inhibitor in the active site of CYP2B4. These findings are consistent with the experimental results, where replacement of residues 114 and 367 led to significant changes in the IC_{50} values.

Identification of Phenylimidazole Derivatives with Enhanced Differential Inhibition of CYP2B4 and CYP2B5. An initial screen of derivatives with substituents at various positions of the phenyl moiety of the phenylimidazole compounds showed that all phenylimidazoles tested were more potent inhibitors of CYP2B4 than of CYP2B5 activity. A chlorine substituent at position 4 of the phenyl moiety of the phenylimidazoles resulted in significantly increased potency of inhibition of CYP2B4 (Table 4). CYP2B4 was 7.5-fold more sensitive to 1-(4-chlorophenyl)imidazole and 12.3-fold more sensitive to 4-(4-chlorophenyl)imidazole than to 1- and 4-phenylimidazole, respectively. Interestingly, 1-(4-chlorophenyl)imidazole was 3.7-fold less potent as an inhibitor of CYP2B5 compared with 1-phenylimidazole. However, 4-(4-chlorophenyl)imidazole was twice as potent for CYP2B5 as the parent compound 4-phenylimidazole. Whereas the IC_{50} values of 1- and 4-phenylimidazole were 5- and 17-fold lower for CYP2B4 than for CYP2B5, the values for 1- and 4-(4-chlorophenyl)imidazole were 130- and 95-fold lower for CYP2B4 than for CYP2B5. CYP2B1 showed not only similar active-site residues involved in inhibition, but all tested phenylimidazole compounds yielded IC_{50} values comparable with CYP2B4. Interestingly, inhibition of the CYP2B4 quadruple mutant and the CYP2B5 quadruple mutant by 1-(4-chlorophenyl)imidazole exhibited the same in-

TABLE 3

Inhibition of CYP2B1 enzymes by 4-phenylimidazole

IC_{50} values are the means of two independent BROD assays performed in duplicate and K_D values were determined as described under *Experimental Procedures*.

CYP2B1	IC_{50}	K_D
	μM	
WT	0.26	0.28
V367L	0.04	N.D.
V363L	0.09	N.D.
V363A	0.31	N.D.
S294T	0.31	N.D.
S294A	0.4	N.D.
L58F-I114F-S294T	0.4	0.57
V367A	6	4.1
L58F-I114F	34	30.5

N.D., not determined.

```
    31         41         51         61         71         81         91
B1: ppgprplpll gnllqldrgg llnsfmqlre kygdvftvhl gprpvvmlcg tdtikealvg qaedfsgrgt
B4: ppgpsplpvl gnllqmdrkg llrsflrlre kygdvftvyl gsrpvvvlcg tdairealvd qaeafsgrgk
B5: ppgppplpvl gnllqmdrkg llrsflrlre kygdvftvyl gsrpvvvlcg tdairealvd qaeafsgrgk
C5: ppgptpfpii gnilqidakd isksltkfse cygpvftvyl gmkptvvlhg yeavkealvd lgeefagtgs
    101        111        121        131        141        151        161
B1: iaviepifke ygvifanger wkalrrfsla tmrdfgmgkr sveeriqeea qclveelrks qgapldptfl
B4: iavvdpifqg ygvifanger wralrrfsla tmrdfgmgkr sveeriqeea rclveelrks kgalldntll
B5: iavvdpifqg ygvifangeh wralrrfsla tmrdfgmgkr sveeriqeea rclveelrks kgalldntll
C5: vpilekvskg lgiafsnakt wkemrrfslm tlrnfgmgkr siedriqeea rclveelrkt naspcdptfi
    171        181        191        201        211        221        231
B1: fqcitaniic sivfgerfdy tdrqflrlle lfyrtfslls sfssqvfeff sgflkyfpga hrqisknlqe
B4: fhsitsniic sivfgkrfdy kdpvflrlld lffqsfslis sfssqvfelf pgflkhfpgt hrqiyrnlqe
B5: fhsvtsniic sivfgkrfdy kdpvflrlld lffqsfslis sfssqvfelf pgflkhfpgt hrqiyrnlqe
C5: lgcapcnvic svifhnrfdy kdeeflklme slnenvrils spwlqvynnf palldyfpgi hktllknady
    241        251        261        271        281        291        301
B1: ildyighive khratldpsa prdfidtyll rmekeksnhh tefhhenlmi sllslffagt etssttlryg
B4: intfigqsve khratldpsn prdfidvyll rmekdksdps sefhhqnlil tvlslffagt ettsttlryg
B5: intfigqtve khratldpsn prdfidvyll rmekdksdps sefhhrnlil tvltlffagt ettsttlryg
C5: iknfimekvk eheklldvnn prdfidcfli kmege---nn leftleslvi avsdlfgagt ettsttlrys
    311        321        331        341        351        361        371
B1: fllmlkyphv aekvqkeidq vigshrlptl ddrskmpytd aviheiqrfs dlvpigvphr vtkdtmfrgy
B4: fllmlkyphv tervqkeieq vigshrppal ddrakmpytd aviheiqrlg dlipfgvpht vtkdtqfrgy
B5: fllmlkyphv tervqkeieq vigshrppal ddrakmpytd aviheiqrlg dlvpfgapht vtkdtqfrgy
C5: lllllkhpev aarvqeeier vigrhrspcm qdrsrmpytd aviheiqrfi dllptnlpha vtrdvrfrny
    381        391        401        411        421        431        441
B1: llpkntevyp ilssalhdpq yfdhpdsfnp ehfldangal kkseafmpfs tgkriclgeg iarnelflff
B4: vipkntevfp vlssalhdpr yfetpntfnp ghfldangal krnegfmpfs lgkriclgeg iartelflff
B5: vipkntevfp vlssalhdpr yfetpntfnp ghfldadgal krnegfmpfs lgkriclgeg iartelflff
C5: fipkgtdiit sltsvlhdek afpnpkvfdp ghfldesgnf kksdyfmpfs agkrmcvgeg larmelflfl
    451        461        471        481
B1: ttilqnfsvs shlapkdidl tpkesgigki pptyqicfsa r
B4: ttilqnfsia spvppedidl tpresgvgnv ppsyqirfla r
B5: ttilqnfsia spvppedidl tpresgvgnv ppsyqirfla r
C5: tsilqnfklq slvepkdldi tavvngfvsv ppsyqlcfip i
```

Fig. 2. Sequence alignment between CYP2B1, CYP2B4, CYP2B5, and CYP2C5 from residue 31 to 491. The changed insertion and the analyzed active-site residues are underlined. The multiple alignment method PileUp in GCG (Genetics Computer Group) was used. The sequence identities are 51.5% between CYP2B1 and CYP2C5, 50.7% between CYP2B4 and CYP2C5, and 50.7% between CYP2B5 and CYP2C5. The four key residues, 114, 294, 363, and 367, are highlighted.

terconversion of sensitivity as observed for 4-phenylimidazole (data not shown). Inhibition of the CYP2B4 quadruple mutant and the CYP2B5 quadruple mutant by 1-(4-chlorophenyl)imidazole yielded IC_{50} values of 5.2 μM and 0.16 μM, respectively. Studies of inhibition by 4-(4-chlorophenyl)imidazole of the androstenedione hydroxylase activities in phenobarbital-induced rat liver microsomes showed 50% inhibition of CYP2B1 activity at a 200 nM inhibitor concentration, whereas CYP2A1, CYP3A1/2, and CYP2C activities were inhibited only in the micromolar range of 4-(4-chlorophenyl)imidazole (data not shown).

Discussion

This study investigated the structural basis of differential inhibition by phenylimidazoles of CYP2B4, CYP2B5, and CYP2B1 using active-site mutants and molecular models. Recent studies have shown that the SRS residues 114, 294, 363, and 367 are critical for regio- and stereospecificity of androstenedione hydroxylation and for the oxidation of several other substrates by CYP2B4 and CYP2B5 (Szklarz et al., 1996). In the present investigation, we have found that these active-site residues are also responsible for differential sensitivity to inhibition by 4-phenylimidazole. Moreover, the simultaneous substitution of the four residues 114, 294, 363, and 367 in 2B5 by the residues of CYP2B4 confers the sensitivity to inhibition of CYP2B4 on CYP2B5 and vice versa. The same interconversion was observed for androstenedione hydroxylase activity (He et al., 1996).

To elucidate the complex role of active-site residues in inhibitor sensitivity, molecular models were used. Initially, 4-phenylimidazole was docked into the active site of CYP2B models based on the bacterial P450s $P450_{cam}$, P450 BM-3, and P450terp (Szklarz et al., 1995). However, these models did not aid the interpretation of our experimental data, especially those on CYP2B5. Very recently, the first mammalian P450, CYP2C5, was crystallized (Williams et al., 2000). The 2B enzymes belong to the same P450 family as CYP2C5, and the sequence identity is high (51.5% for CYP2B1; 50.7%

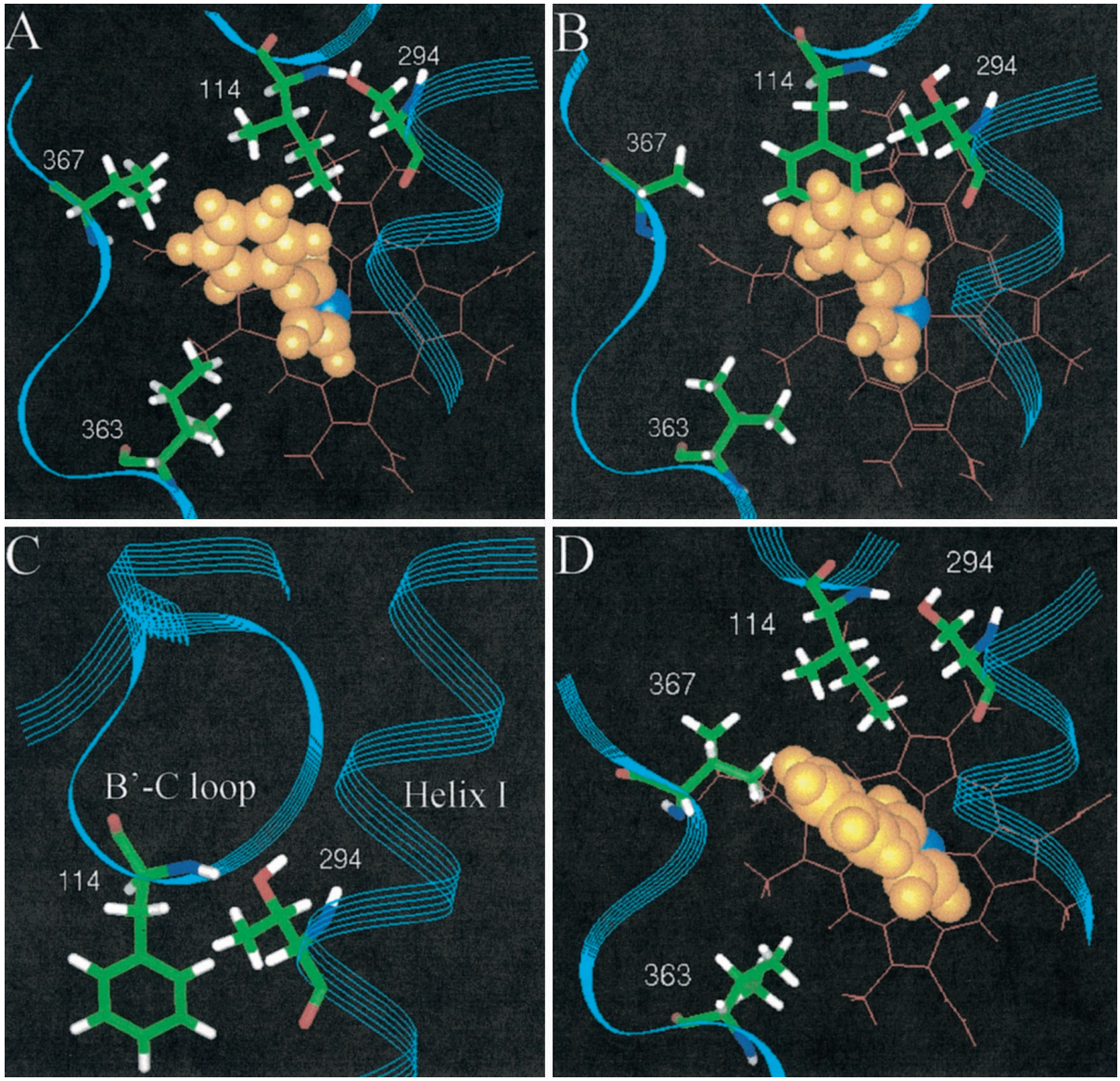

Fig. 3. 4-phenylimidazole docked into the active site of the CYP2B models. A, CYP2B4. B, CYP2B5. C, the interaction between the B′-C loop and helix I in CYP2B5. D, CYP2B1. The heme is shown in red. 4-Phenylimidazole is shown in yellow with the nitrogen in blue pointing to the heme iron.

for CYP2B4 and CYP2B5), as opposed to 15 to 20% with the bacterial P450s. Therefore, the homology modeling of CYP2B1, CYP2B4, and CYP2B5 based on the crystal structure of CYP2C5 provides a significant refinement compared with 2B models based on the bacterial P450s.

The first novel insight gained with the new 2B models was

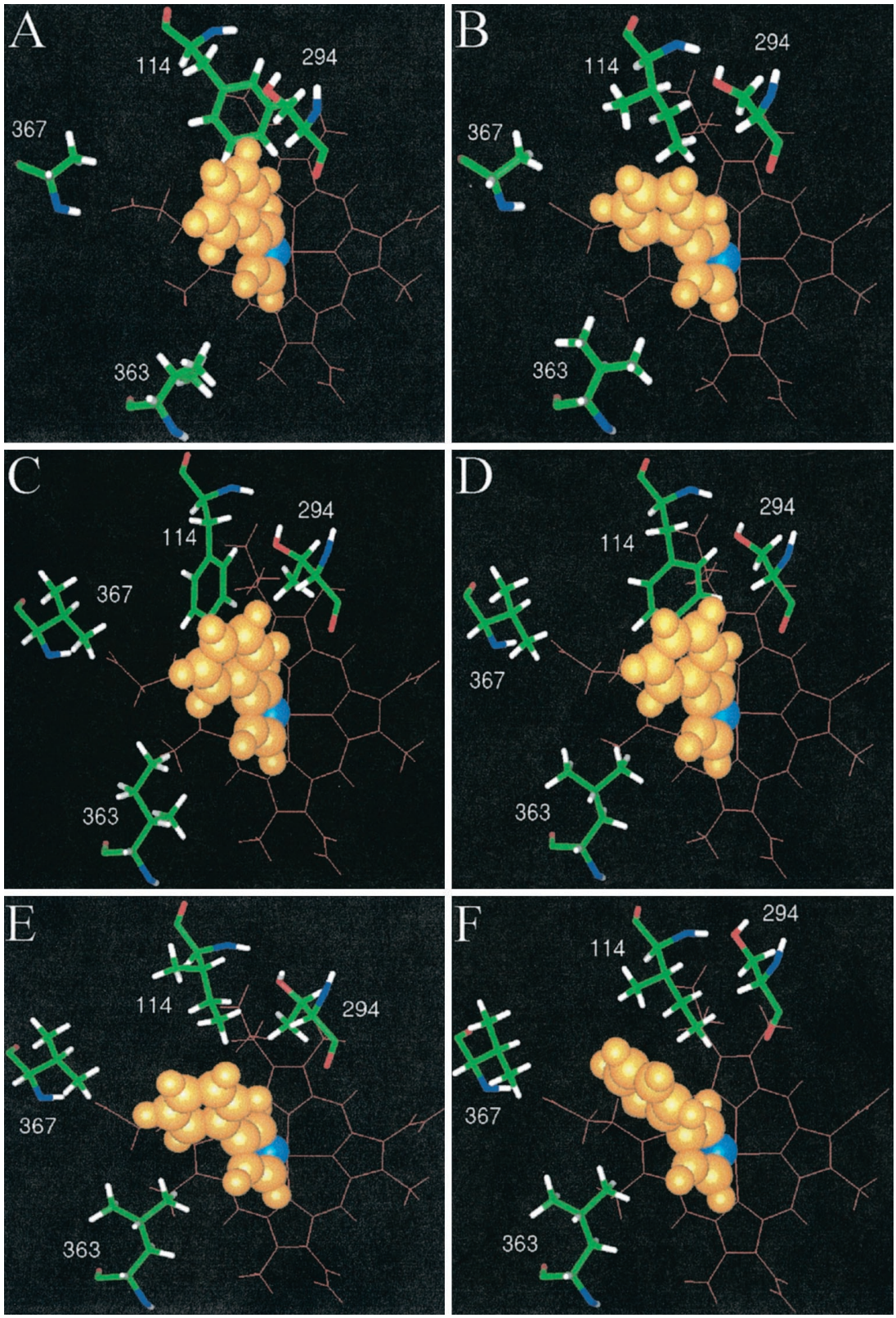

Fig. 4. 4-Phenylimidazole (4-P) docked into the active site of the CYP2B5 mutants. A, 2B5 T294S (distance from 4-P: 114, 3.5Å; 294, 3.7 Å; 363, 5.6 Å; 367, 9.7 Å). B, 2B5 F114I-T294S (distance from 4-P: 114, 3.6 Å; 294, 5.1 Å; 363, 5.2 Å; 367, 6.9 Å). C, 2B5 V363I-A367V (distance from 4-P: 114, 3.5 Å; 294, 4 Å; 363, 5.1 Å; 367, 6.6 Å). D, 2B5 T294S-V363I-A367V (distance from 4-P: 114, 3.5 Å; 294, 4.2 Å; 363, 4.2 Å; 367, 6.6 Å); E, 2B5 F114I-V363I-A367V (distance from 4-P: 114, 3.5 Å; 294, 5 Å; 363, 4.1 Å; 367, 5.1 Å). F, 2B5 F114I-T294S-V363I-A367V (distance from 4-P: 114, 3.8 Å; 294, 6.4 Å; 363, 4.1 Å; 367, 5.1 Å).

provided by docking 4-phenylimidazole into CYP2B4 and from the analysis of active-site mutants of CYP2B4. Both inhibition studies and molecular modeling indicate that CYP2B4 residues 114 and 367 play a critical role in sensitivity to 4-phenylimidazole (Table 1, Fig. 3A). A single Val 367-to-Ala substitution causes a 10-fold decrease in sensitivity to a level comparable with that of CYP2B5. The Ile residue at position 114 may be of similar importance for the sensitivity to inhibition of 2B4. The 3D model shows that residue 114 is as near as residue 367 to the phenyl moiety of 4-phenylimidazole. Simultaneous substitution of Ile 114 with the bulkier aromatic residue Phe and of Ser 294 with Thr leads to a significant decrease in sensitivity to inhibition, suggesting that the side chain of phenylalanine may cause steric hindrance. The side chain of position 114 was also observed to be crucial for the selective androstenedione hydroxylation in 2B4 and 2B5 (Szklarz et al., 1996). However, the interaction of the substrate with this residue could not be explained by molecular modeling based on bacterial P450s. Residue 114 is located in the B′-C-loop, a segment known to differ significantly between the bacterial P450s and the mammalian CYP2 family. Therefore, for the first time the crucial position of this residue for inhibitor and substrate interactions could be explained.

Another remarkable and intriguing new feature was observed in the model of CYP2B5 and the inhibition results with the active-site mutants. Similar to CYP2B4, the side chain of residue 114 is also crucial for the inhibition of CYP2B5 by 4-phenylimidazole. Docking of 4-phenylimidazole into the active site of CYP2B5 indicates that binding of the compound may be impeded by steric hindrance from the phenyl ring of Phe 114 (Fig. 3B). This finding may explain the significantly higher IC_{50} value of 4-phenylimidazole for CYP2B5 compared with that of CYP2B4 (Table 2). In contrast to CYP2B4, none of the single mutations in CYP2B5 could confer sensitivity to inhibition similar to CYP2B4 WT. Interestingly, substitution of Thr 294 with Ser causes a 10-fold increase in the IC_{50} value. Upon alteration of residue 294, the phenyl ring of Phe 114 changes its position, as indicated by comparison of the 3D models of this mutant and CYP2B5 WT (Figs. 4A and 3B). Consequently, the π-π interaction of the two parallel phenyl rings in CYP2B5 WT disappears. The substitution of Phe 114 with Ile favors a higher sensitivity to inhibition by removing the steric hindrance for 4-phenylimidazole. However, the IC_{50} value of CYP2B5 F114I-T294S remains higher than that of the WT, perhaps because of the loss of the π-π interaction (Table 2; Fig. 4B). The substitution of Val 363 and Ala 367 with the larger residues Ile and Val, respectively, may enhance the hydrophobic interactions with 4-phenylimidazole (Fig. 4C). However, in CYP2B5 mutants V363I-A367V and T294S-V363I-A367V, steric hindrance from Phe 114 could prevent the phenylimidazole compound from tighter binding. Subsequently, no significantly higher inhibition sensitivity for these two mutants was observed compared with the WT, despite the increased hydrophobic interactions of Ile 363 and Val 367 with the compound (Fig. 4, C and D; Table 2). Both the free movement of the compound in the active site achieved by the substitution of Phe 114 with Ile and the hydrophobic interactions of the Ile 363 and Val 367 with the compound are necessary to significantly increase the sensitivity to 4-phenylimidazole (Fig. 4E; Table 2). However, substitution of all four residues by the corresponding residues of CYP2B4 is required to achieve an inhibition sensitivity similar to that of CYP2B4 (Fig. 4F; Table 2). The experimental and modeling results with CYP2B5 and its mutants demonstrated that the exact architecture of the inhibitor binding site is determined not only by individual contributions from key inhibitor contact residues, but also by residue-residue interactions. This intriguing interplay of active-site residues, especially involving residues 114 and 294, was previously inferred from a study of androstenedione hydroxylase specificity of CYP2B4 and CYP2B5 (He et al., 1996). As the model available at that time was based on bacterial P450s, the mutagenesis data could not fully be explained.

A further interesting point is the extrapolation of the findings above to rat CYP2B1. Previous investigations of the CYP2B enzymes have already shown that residues important for activities of CYP2B4 and CYP2B5 are also essential for other members of the 2B family (He et al., 1994; Szklarz et al., 1995; Lewis and Lake, 1997). Inhibition studies and the 3D models demonstrated striking similarities between CYP2B4 and CYP2B1 (Tables 1, 3, and 4). Val 367 plays a major role for sensitivity to inhibition by 4-phenylimidazole in CYP2B1 as well as in CYP2B4. In CYP2B1 and CYP2B4, the sensitivity to inhibition decreases significantly upon replacement of Val 367 with the smaller Ala residue. To further investigate the importance of residue 367, we tested CYP2B1 V367L, which exhibited a significant lower IC_{50} value than the wild-type enzyme, presumably because of tighter hydrophobic binding with the longer side chain of Leu. These findings were supported by the 3D model of CYP2B1, which showed that Val 367 is substantially closer to 4-phenylimidazole than any other of the four investigated residues (Fig. 3D). As observed for CYP2B4 and CYP2B5, the side chain of residue 114 may be also of great importance for the sensitivity to inhibition in CYP2B1. Mutant I114F mutant did not express. To achieve reasonable expression and activity, CYP2B1 L58F-I114F was constructed. Consistent with the results obtained for CYP2B4 and CYP2B5, this mutant showed a dramatic decrease in sensitivity. However, the additional Ser 294-to-Thr substitution restored sensitivity to inhibition. This finding is consistent with the 114–294 residue interaction observed in CYP2B5.

Interestingly, substantially higher selectivity for CYP2B4 over CYP2B5 was achieved with a chlorine substituent on the phenyl moiety. These findings suggest 1- and 4-(4-chlorophenyl)imidazole as useful inhibitors to distinguish between CYP2B4 and CYP2B5. As already observed for 4-phenylimidazole, CYP2B1 yielded about the same IC_{50} values as CYP2B4 for all tested phenylimidazole compounds. Although

TABLE 4

Inhibition of CYP2B4, 2B5 and 2B1 by phenylimidazole derivatives

Values are the means of two independent experiments performed in duplicate and conducted as described under *Experimental Procedures*. Data for CYP2B4 and 2B1 are determined by BROD assay. Data for CYP2B5 are determined by PROD assay.

Compounds	IC_{50}		
	CYP2B4	CYP2B5	CYP2B1
		μM	
1-Phenylimidazole	0.90	4.2	0.59
1-(4-Chlorophenyl)imidazole	0.12	15.6	0.08
4-Phenylimidazole	0.49	8.4	0.26
4-(4-Chlorophenyl)imidazole	0.04	3.8	0.07

the orientation of the phenyl moiety of 4-phenylimidazole in the 3D models of CYP2B4 and CYP2B1 is different, the similar sensitivity to inhibition of these two enzymes might be caused by the same residues at positions 114 and 367.

In conclusion, the results of the present investigation reveal that the active-site residues 114, 294, 363, and 367 in CYP2B4, 2B5, and 2B1 are crucial for reversible inhibition, as already observed for substrate specificity and mechanism-based inactivation (He et al., 1992, 1994, 1995; Strobel et al., 1999). Furthermore, molecular models based on the crystal structure of CYP2C5 are of great value to explain the complex molecular basis of reversible inhibition by phenylimidazoles. These findings may contribute to a considerably better understanding of the CYP2B enzymes and to the design of a selective human CYP2B6 inhibitor. Knowledge of the residues responsible for inhibition and of residue-residue interactions may also help to modulate chemical structures to avoid inhibition and resulting drug-drug interactions. Moreover, because the five main CYP2 subfamilies possess overlapping structure-function and substrate specificities (Lewis, 1998), the findings presented here may apply to other members of the CYP2 family.

Acknowledgments

We thank Dr. Tammy Domanski for kindly providing several CYP2B1 mutants.

References

Augustinsson KB (1948) Cholinesterases: A study in comparative enzymology. *Acta Physiol Scand* **15:**52–60.
Chang YT, Stiffelman OB, Vakser IA, Loew GH, Bridges A and Waskell L (1997) Construction of a 3D model of cytochrome P450 2B4. *Protein Eng* **10:**119–129.
Copeland RA (2000) Protein-ligand binding equilibria, in *Enzymes* (Copeland RA ed) pp 76–108, John Wiley & Sons, New York.
Cosme J and Johnson EF (2000) Engineering microsomal cytochrome P450 2C5 to be a soluble, monomeric enzyme. Mutations that alter aggregation, phospholipid dependence of catalysis, and membrane binding. *J Biol Chem* **275:**2545–2553.
Dai R, Pincus MR and Friedman FK (1998) Molecular modeling of cytochrome P450 2B1: Mode of membrane insertion and substrate specificity. *J Protein Chem* **17:**121–129.
Dai R, Pincus MR and Friedman FK (2000) Molecular modeling of mammalian cytochrome P450s. *Cell Mol Life Sci* **57:**487–499.
de Groot MJ, Ackland MJ, Horne VA, Alex AA and Jones BC (1999) Novel approach to predicting P450-mediated drug metabolism: Development of a combined protein and pharmacophore model for CYP2D6. *J Med Chem* **42:**1515–1524.
Halpert JR (1995) Structural basis of selective cytochrome P450 inhibition. *Annu Rev Pharmacol Toxicol* **35:**29–53.
Harlow GR and Halpert JR (1997) Alanine-scanning mutagenesis of a putative substrate recognition site in human cytochrome P450 3A4. *J Biol Chem* **272:**5396–5402.
He YA, Balfour CA, Kedzie KM and Halpert JR (1992) Role of residue 478 as a determinant of the substrate specificity of cytochrome P450 2B1. *Biochemistry* **31:**9220–9226.
He YA, Luo Z, Klekotka PA, Burnett VL and Halpert JR (1994) Structural determinants of cytochrome P450 2B1 specificity: Evidence for five substrate recognition sites. *Biochemistry* **33:**4419–4424.
He YQ, He YA and Halpert JR (1995) *Escherichia coli* expression of site-directed mutants of cytochrome P450 2B1 from six substrate recognition sites: Substrate specificity and inhibitor selectivity studies. *Chem Res Toxicol* **8:**574–579.
He YQ, Szklarz GD and Halpert JR (1996) Interconversion of the androstenedione hydroxylase specificities of cytochrome P450 2B4 and 2B5 upon simultaneous site-directed mutagenesis of four key substrate recognition residues. *Arch Biochem Biophys* **335:**152–160.
John GH, Hasler JA, He YA and Halpert JR (1994) *Escherichia coli* expression and characterization of cytochromes P450 2B11, 2B1, and 2B5. *Arch Biochem Biophys* **314:**367- 375.
Kobayashi Y, Fang X, Szklarz GD and Halpert JR (1998) Probing the active site of cytochrome P450 2B1: Metabolism of 7-alkoxycoumarins by the wild type and five site-directed mutants. *Biochemistry* **37:**6679–6688.
Lewis DF (1998) The CYP2 family: Models, mutants and interactions. *Xenobiotica* **28:**617–661.
Lewis DF and Lake BG (1997) Molecular modelling of mammalian CYP2B isoforms and their interaction with substrates, inhibitors and redox partners. *Xenobiotica* **27:**443–478.
Murray M (1987) Mechanisms of the inhibition of cytochrome P-450-mediated drug oxidation by therapeutic agents. *Drug Metab Rev* **18:**55–81.
Murray M and Wilkinson CF (1984) Interactions of nitrogen heterocycles with cytochrome P- 450 and monooxygenase activity. *Chem-Biol Interact* **50:**267–275.
Omura T and Sato R (1964) The carbon monoxide-binding pigment of liver microsomes. *J Biol Chem* **239:**2379–2387.
Paulsen MD and Ornstein RL (1991) A 175-psec molecular dynamics simulation of camphor- bound cytochrome P-450$_{cam}$. *Proteins* **11:**184–204.
Paulsen MD and Ornstein RL (1992) Predicting the product specificity and coupling of cytochrome P450$_{cam}$. *J Comput Aided Mol Des* **6:**235–252.
Payne VA, Chang YT and Loew GH (1999) Homology modeling and substrate binding study of human CYP2C9 enzyme. *Proteins* **37:**176–190.
Pelkonen O, Maenpaa J, Taavitsainen P, Rautio A and Raunio H (1998) Inhibition and induction of human cytochrome P450 (CYP) enzymes. *Xenobiotica* **28:**1203–1253.
Poulos TL and Howard AJ (1987) Crystal structures of metyrapone-and phenylimidazole- inhibited complexes of cytochrome P-450$_{cam}$. *Biochemistry* **26:**8165–8174.
Shenkin PS, Yarmush DL, Fine RM, Wang H and Levinthal C (1987) Predicting antibody hypervariable loop conformation. I. Ensembles of random conformations for ringlike structures. *Biopolymers* **26:**2053–2085.
Strobel SM and Halpert JR (1997) Reassessment of cytochrome P450 2B2: Catalytic specificity and identification of four active site residues. *Biochemistry* **36:**11697–11706.
Strobel SM, Szklarz GD, He YQ, Foroozesh M, Alworth WL, Roberts ES, Hollenberg PF and Halpert JR (1999) Identification of selective mechanism-based inactivators of cytochrome P- 450 2B4 and 2B5, and determination of the molecular basis for differential susceptibility. *J Pharmacol Exp Ther* **290:**445–451.
Szklarz GD, He YA and Halpert JR (1995) Site-directed mutagenesis as a tool for molecular modeling of cytochrome P450 2B1. *Biochemistry* **34:**14312–14322.
Szklarz GD, He YQ, Kedzie KM, Halpert JR and Burnett VL (1996) Elucidation of amino acid residues critical for unique activities of rabbit cytochrome P450 2B5 using hybrid enzymes and reciprocal site-directed mutagenesis with rabbit cytochrome P450 2B4. *Arch Biochem Biophys* **327:**308–318.
Williams PA, Cosme J, Sridhar V, Johnson EF and McRee DE (2000) Mammalian microsomal cytochrome P450 monooxygenase: Structural adaptions for membrane binding and functional diversity. *Mol Cell* **5:**121–131.

Send reprint requests to: Dr. Margit Spatzenegger, Department of Pharmacology and Toxicology, University of Texas Medical Branch at Galveston, 301 University Blvd., Galveston, TX 77555-1031. E-mail: maspatze@utmb.edu